Supporting Information for

Effect of Curing Reaction Types on the Structures and Properties of Acetylene-Containing Thermosets: Towards Optimization of Curing Strategy

Junli Zhu, Liquan Wang*, Jiaping Lin*, Lei Du, Qixin Zhuang

Shanghai Key Laboratory of Advanced Polymeric Materials, Key Laboratory for Ultrafine Materials of Ministry of Education, Frontiers Science Center for Materiobiology and Dynamic Chemistry, School of Materials Science and Engineering, East China University of Science and Technology, Shanghai 200237, China

Corresponding Authors

Tel: +86-21-64253370.

E-mail: lq_wang@ecust.edu.cn (L.W.) and jlin@ecust.edu.cn (J.L.).

Contents

1. Procedure for the Curing of Resins in MD Simulations

The procedure for simulating the curing of resins in MD simulations is shown in Figure S1. Uncured resins were placed in a simulation box using an Amorphous Cell modulus. The system was subjected to geometry optimization, and molecular dynamics simulation under the *NPT* ensembles was performed successively. The equilibrium configuration was used for the following crosslinking strategies. Pairs of reactive atoms within the cut-off distance were searched and connected by forming new bonds. Bonds and neighboring atoms for the reacted atoms were adjusted, and the total system was subjected to the geometry optimization and 10-ps *NPT* simulations to eliminate internal stress stemming from the crosslinking. The relaxation time is sufficient for removing unrealistic distortions. Cyclotrimerization, Diels-Alder reaction, and radical polymerization were considered in this procedure. The above simulations were repeated until the target conversion was reached, or there was no new pair of reactive atoms generated within the maximum cut-off distance. To build reasonable crosslinked polymers in a suitable computational time, we increased the cut-off distance from 4 Å to 12 Å in this study. Such an approach has been commonly used in molecular dynamics simulations to construct the crosslinked polymer networks[S1-S6]. Since the present study does not focus on the properties related to the reaction time, this strategy is suitable for building crosslinked polymers with a reasonable time by molecular dynamics simulations.

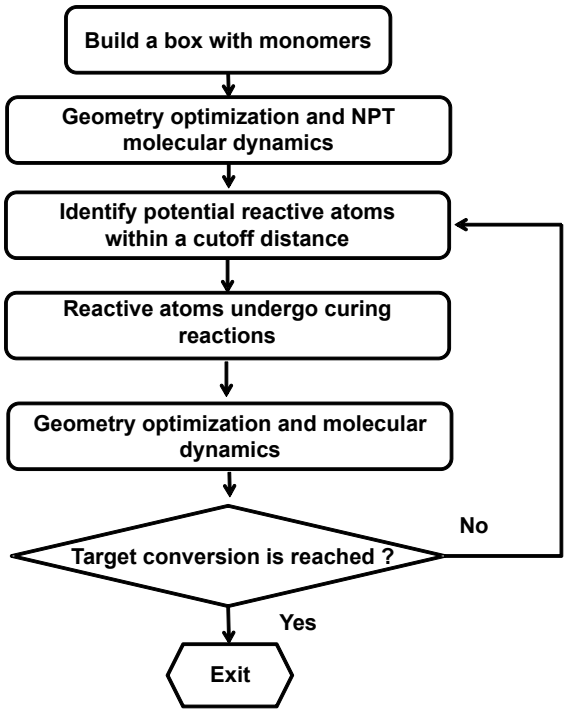

Figure S1. Crosslinking flowchart in the MD simulations.

In the curing process, several methods have been adopted to construct the polymer networks without unrealistic distortions. The maximum bond energy in the cured system during the curing was monitored to avoid ring spearing. The abrupt increase of the maximum bond energy indicates the occurrence of the ring spearing, as shown in Figure S2. The cured systems with ring spearing were abandoned.

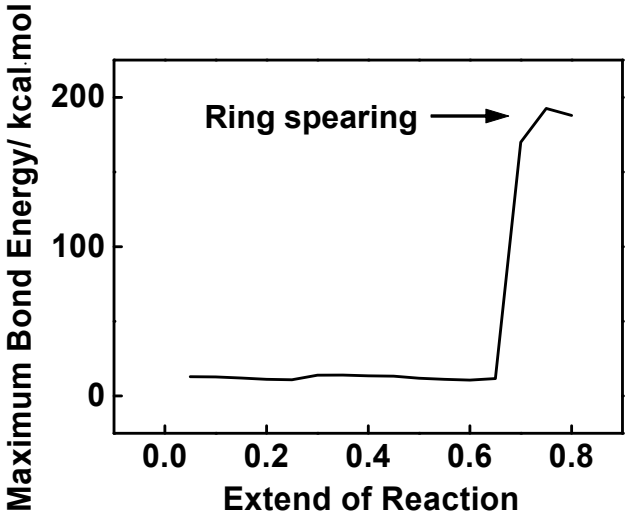

Figure S2. The maximum bond energy in the system as a function of the extent of reaction

In addition, we analyzed the length distributions of all the bonds in the cured systems to check the sufficient relaxation of cured systems. Figure S3 shows the bond length distributions in the cured systems with a reaction extent of 0.8. Compared with the distribution curve of the uncured system, the smaller peaks at 1.2 Å in the curves of the cured systems indicates the consumption of the alkynyl groups and the difference in the curves for the cured and uncured systems in the range of 1.4 Å to 1.6 Å suggests the formation of the new cured structures. No stretched bonds have been found in the bond length distributions in the cured systems, which means that unrealistic distortions have been avoided.

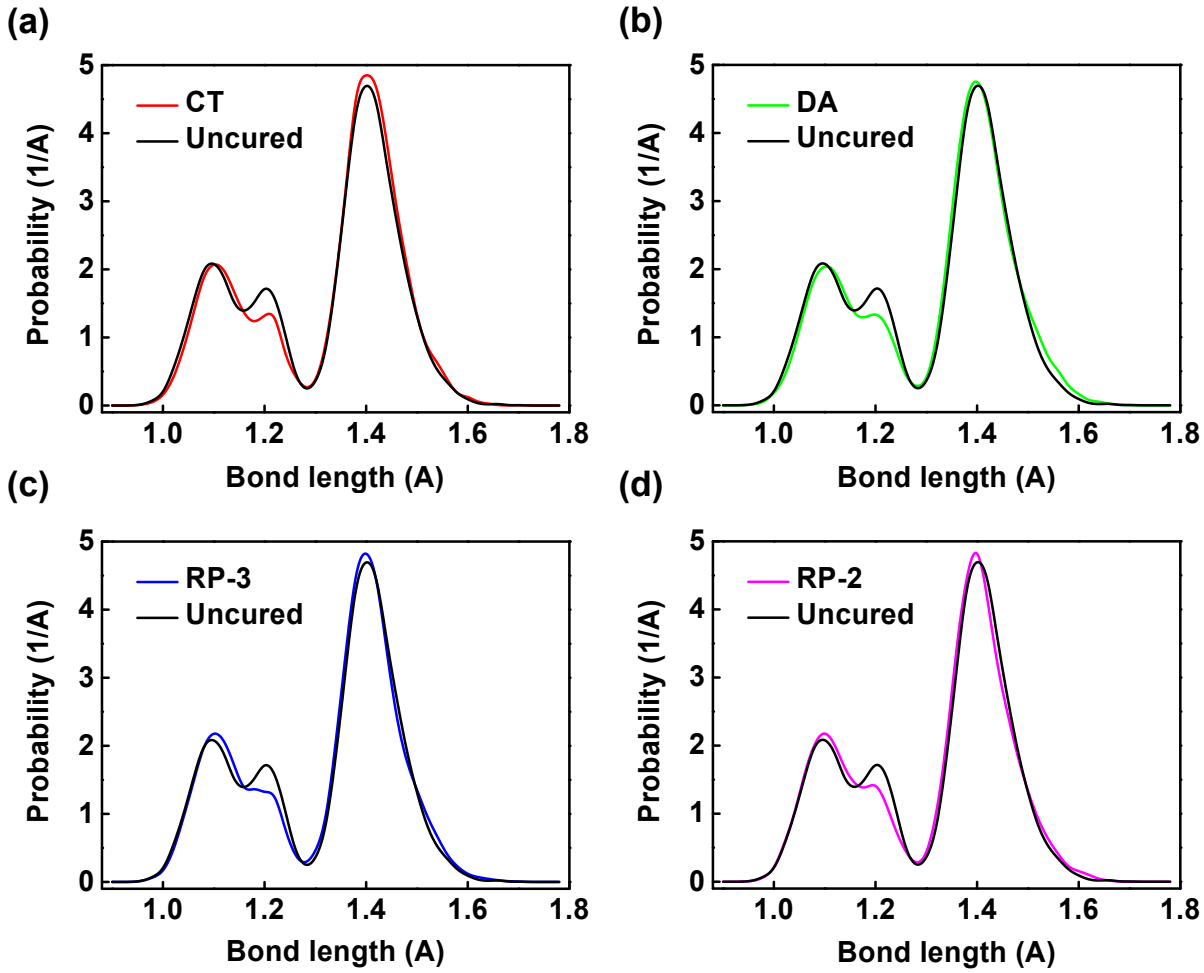

Figure S3. The length distributions of all the bonds in the cured systems for (a) CT, (b) DA, (c) RP-3, and (d) RP-2 at the extent of reaction of 0.8.

Our previous density functional theory computation shows that the major cyclotrimerization pathway includes the dimerization of two arylacetylenes into a diradical intermediate, which then undergoes the intramolecular couplings to strained cyclic allene and cyclobutadiene, followed by the evolution into naphthalenic dimer and benzenic trimer[S7]. The stress can be alleviated in the stepwise reaction. However, such a process cannot be achieved in molecular dynamics simulations. In our work, the crosslinking reaction was simulated by applying a harmonic potential to bring reactants together in a single step. Only one reaction takes place at a time, and enough time was taken for relaxing the chain after each crosslink. Such a method could mimic the stepwise alleviation of stresses from crosslinking.

2. Average Molecular Weight of the Cured Polymers

We have examined the number-average molecular weight (M_n) of polymers as a function of the extent of reaction. The result is shown in Figure S4. Since three alkynyl groups are involved in each CT/RP-3 reaction and only two alkynyl groups are included in each DA/RP-2 reaction, the average molecular weights of DA and RP-2 systems are lower than those of CT and RP-3 systems.

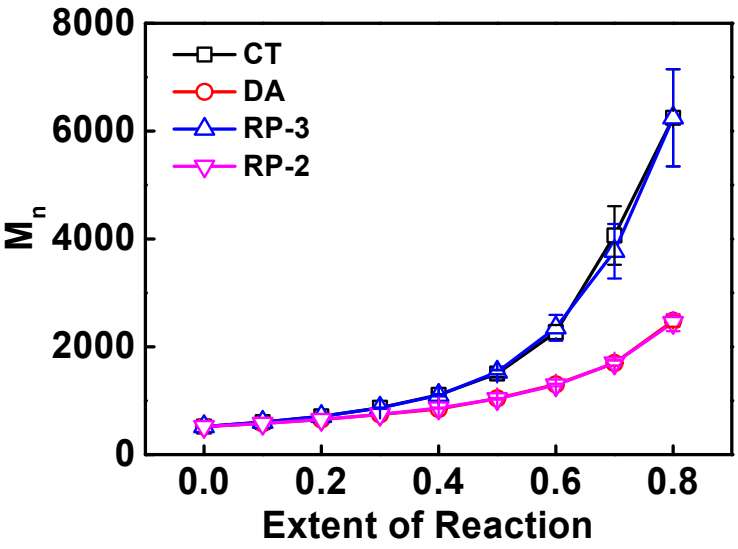

Figure S4. The number-average molecular weight (M_n) of polymers as a function of the extent of reaction.

3. Radial Distribution Function

Figure S5 shows the pair distribution function $g(r)$ for molecule pairs in the cured polymers. As shown, compared with the linear polymers obtained by DA and RP-2, the polymers crosslinked by CT and RP-3 have an apparent distinction in $g(r)$ with intermolecular distance in the range of 4 to 6 Å. The intermolecular distances in the polymer networks cured by CT and RP-3 are shorter than those in the DA and RP-2 systems. The results indicate that the crosslinking effects of CT and RP-3 decrease the intermolecular distance between monomers and increase the density of the cured resins.

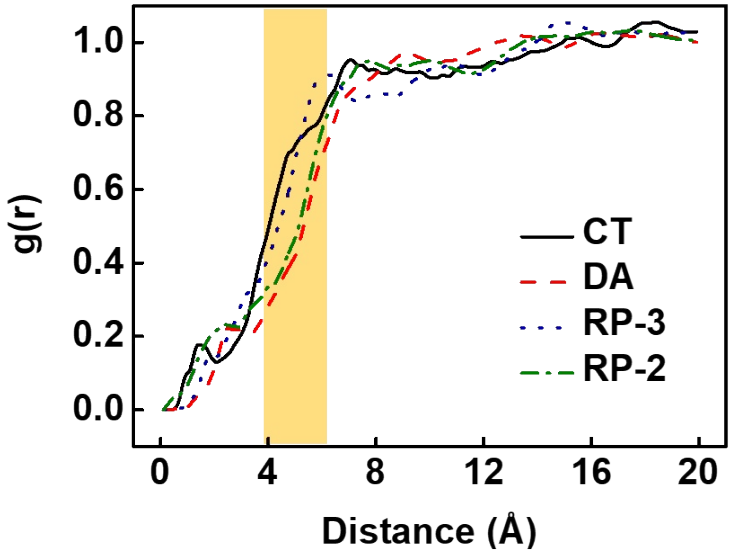

Figure S5. Radial distribution function $g(r)$ for molecule pairs in the cured polymers.

4. Curing Process for the Resins of Different Kinds of Reactions

Figure S6 shows the plots of the conversion of monomers as a function of the extent of the reaction. As shown, the four reaction systems exhibit a similar variation of the conversion. The number of uncured molecules decreases, and the number of fully reacted (cured at two ends) molecules increases in the entire process. The number of partly reacted (cured at one end) molecules first increases and then decreases with increasing the reaction extent. The maximum number of one-end cured resins appears at the reaction extent of *ca.* 0.5.

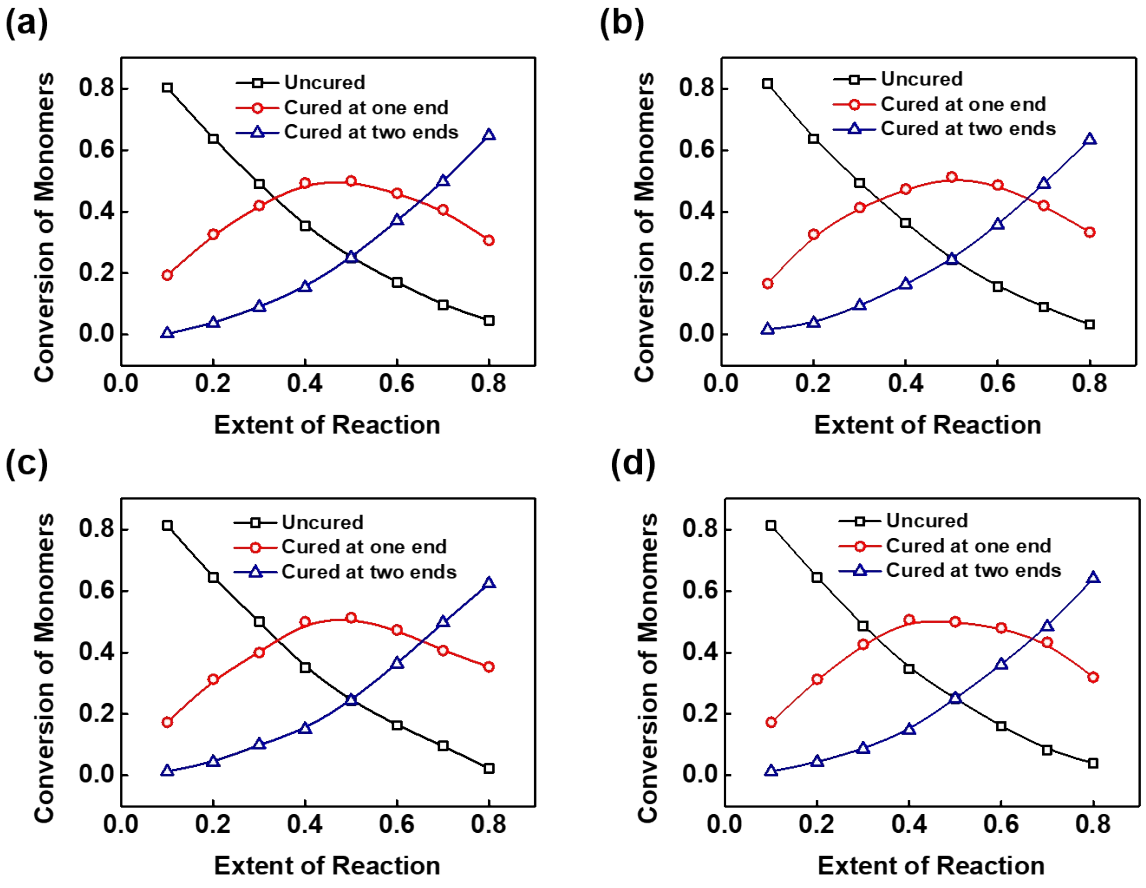

Figure S6. Plots of the conversion of monomers as a function of the extent of the reaction for the resins under the reactions of (a) cyclotrimerization, (b) Diels-Alder reaction, (c) free radical reactions by three alkynes, and (d) free radical reactions by two alkynes.

5. Variations of the Constitutes of Potential Energies

Figure S7 shows the variations of bond energy, angle energy, torsion energy, and non-bond energy as a function of the conversion. As shown, the bond energy (Figure S7a), the angle energy (Figure S7b), the torsion energy (Figure S7c), and the nonbonded interaction energy (Figure S7d) increases with the increase in the conversion. Among the constitutes of potential energies, the torsion energy plays a dominant role in the increase in total potential energy (see Figure S7c). During the curing process, the degree of structural restriction increases due to the formation of new bonds, leading to an increase of torsion energy. Among the four curing reactions, the increase in torsion energy for CT is significantly higher than those for other curing types. For the CT, three molecules cyclotrimerize into a rigid benzene ring, which significantly increases the stiffness of the system and the torsion energy.

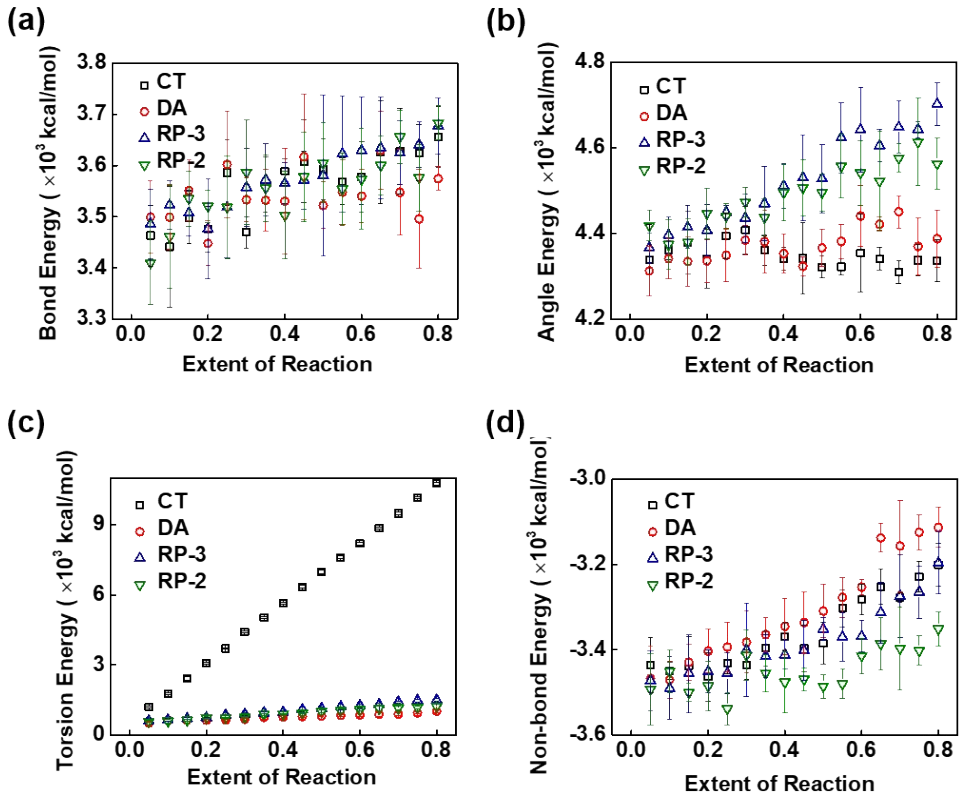

Figure S7. Variations of (a) bond energy, (b) angle energy, (c) torsion energy, and (d) non-bond energy as a function of the conversion.

6. Combined Effects of Various Curing Reactions

We proposed two curing procedures for acetylene-terminated polyimides in which the curing temperature is varied. In the first curing procedure, the acetylene-terminal polyimides are cured at a low temperature (about 150~160°C). In the second curing procedure, the acetylene-terminal polyimides are cured first at a low temperature (about 150~160°C) and then at a high temperature (about 200°C).

As different curing reactions (including radical polymerization, cyclotrimerization, and Diels-Alder reaction) are involved in the two curing procedures, the reaction probability for each reaction needs to be known. We calculated the probabilities of the reactions in MD simulations using the following expression[S8]:

$$P_{\mathrm{r}}(t) = A\exp(-E_{\mathrm{a}} / k_{\mathrm{B}}T)\frac{[M](t)}{[M_0]} \tag{S1}$$

where $P_r(t)$ is the probability for the reaction in MD simulations; A is a modifying factor; E_{a} is the activation energy of the reaction obtained from the DFT calculations[S7]; T is the reaction temperature; $[\mathrm{M}_0]$ is the concentration of the reactive units at the beginning, and $[M](t)$ is the concentration of the reactive units at the specific time.

As the second curing procedure is a two-stage curing process, the conversion at the first stage (low-temperature curing) can be varied, which can be realized by changing the curing time in experiments. The curing time at low temperatures in experiments is usually shorter than the gel time of the resin for easy processing. Therefore, we designed the second curing procedure as follows: the resin was first cured at a low temperature before the gel point was reached, and then the resin was adequately cured at a high temperature. In MD simulations, we determined the conversion at the gel point by analyzing the molecular weights of the fragments in the cured polymer.[S9]

References

[S1]J. Zhu, M. Chu, Z. Chen, L. Wang, J. Lin and L. Du, *Chem. Mater.*, 2020, **32**, 4527-4535.

[S2]D. R. Heine, G. S. Grest, C. D. Lorenz, M. Tsige and M. J. Stevens, *Macromolecules*, 2004, **37**, 3857-3864.

[S3]V. Varshney, S. S. Patnaik, A. K. Roy and B. L. Farmer, *Macromolecules*, 2008, **41**, 6837-6842.

[S4]N. B. Shenogina, M. Tsige, S. S. Patnaik and S. M. Mukhopadhyay, *Macromolecules*, 2012, **45**, 5307-5315.

[S5]C. Wu and W. Xu, *Polymer*, 2006, **47**, 6004-6009.

[S6]S. Masoumi, B. Arab and H. Valipour, *Polymer*, 2015, **70**, 351-360.

[S7]Z. Chen, L. Wang, J. Lin and L. Du, *Phys. Chem. Chem. Phys.*, 2020**, 22**, 6468 - 6477.

[S8]H. Liu, Y.-L. Zhu, Z.-Y. Lu and F. Müller-Plathe, *J. Comput. Chem.*, 2016, **37**, 2634-2646.

[S9]C. Li and A. Strachan, *J. Polym. Sci., Part B: Polym. Phys.*, 2015, **53**, 103-122.